HHS Public Access

Author manuscript

Sci Signal. Author manuscript; available in PMC 2021 August 02.

Published in final edited form as:

Sci Signal. ; 14(668): . doi:10.1126/scisignal.abc4479.

A disease-associated mutation that weakens ZAP70 autoinhibition enhances responses to weak and self ligands

Lin Shen[1], **Mehrdad Matloubian**[1], **Theresa A. Kadlecek**[1,2], **Arthur Weiss**[1,2,*]

[1]Rosalind Russell and Ephraim P. Engleman Rheumatology Research Center, Division of Rheumatology, University of California, San Francisco, CA 94143, USA.

[2]Howard Hughes Medical Institute, University of California, San Francisco, CA 94143, USA.

Abstract

The cytoplasmic kinase ZAP70 is critical for T cell antigen receptor (TCR) signaling. The R360P mutation in ZAP70 is responsible for an early onset familial autoimmune syndrome. The structural location and biochemical signaling effects of the R360P mutation are consistent with weakening of the autoinhibitory conformation of ZAP70. Mice with a ZAP70 R360P mutation and polyclonal TCR repertoires exhibited relatively normal T cell development but showed evidence of increased signaling. Additionally, the R360P mutation resulted in enhanced follicular helper T cell expansion after LCMV infection. To eliminate the possibility of a TCR repertoire shift, the OTI transgenic TCR was introduced into R360P mice, which resulted in enhanced T cell responses to weaker stimuli, including weak agonists and a self-peptide. These observations suggest that disruption of ZAP70 autoinhibition by the R360P mutation enables increased mature T cell sensitivity to self-antigens that would normally be ignored by wild-type T cells, a mechanism that may contribute to the break of tolerance in human patients with R360P mutation.

Introduction

Dysregulation in T cell antigen receptor (TCR) signaling plays critical roles in the pathogenesis of autoimmune diseases (1). ZAP70 (ζ- associated protein of 70 kDa) is a cytoplasmic protein tyrosine kinase that directly interacts with the stimulated TCR complex and is required for activating many downstream signaling pathways in T cells (2, 3). The engagement of the TCR with a peptide MHC (pMHC) complex is transmitted to the cytoplasm through the immunoreceptor tyrosine-based activation motifs (ITAMs) present in the cytoplasmic tails of the CD3 heterodimers and the ζ homodimer. The two tyrosine residues in each ITAM are phosphorylated by Lck, which is non-covalently associated with the coreceptors CD4 or CD8 (2, 4–6). Unphosphorylated ZAP70 is then recruited to doubly phosphorylated ITAMs but remains in an unphosphorylated autoinhibited state. If the TCR

*Corresponding author: arthur.weiss@ucsf.edu.

Author contributions: L.S. and A.W. designed the project. L.S., M.M, and T.A.K performed experiments. L.S, M.M, and A.W. analyzed the data. L.S. and A.W. wrote the manuscript. All authors contributed to the editing of the manuscript.

Competing interests: The authors declare that they have no competing interests.

Data and materials availability: All data needed to evaluate the conclusions in the paper are present in the paper or the Supplementary Materials.

only engages self pMHC complexes in vivo, the dwell time of the interaction is thought to be insufficient for full activation. The prolonged dwell time of agonist pMHC complexes with the TCR induces Lck-mediated phosphorylation of ZAP70 at Tyr^{315}, Tyr^{319} and Tyr^{493}, fully relieving the autoinhibited state, and allowing the kinase to adopt a fully active conformation (2, 4–6). Active ZAP70 phosphorylates at least two scaffold proteins, LAT and SLP-76, leading to the recruitment and activation of effector proteins that activate pathways that induce cytokine production, T cell proliferation and differentiation (2, 4–6).

Complete deficiency or loss of function of ZAP70 has been associated with combined immunodeficiency in humans and mice (7–10). Several mutations in *Zap70* have been associated with autoimmunity in mice (11–13) and in humans (14). Two siblings who were compound heterozygotes for two missense mutations R192W and R360P in *ZAP70* developed a severe autoimmune syndrome by age 3, characterized by bullous pemphigoid, proteinuria, and inflammatory colitis, and one child also developed hemophilia due to an autoantibody to factor VIII (14). The siblings' parents and sister were healthy. Cell line data showed that the R192W mutation, located in the C-SH2 domain, leads to impaired binding of the mutant ZAP70 to phosphorylated ζ-chain, essentially acting as a loss-of-function allele. The R360P mutation is located in the N-lobe of the catalytic domain and based on structural analysis, could interfere with the autoinhibitory mechanism (14). Data from ZAP70-deficient P116 Jurkat cells transiently overexpressing wild type (WT) or mutant *ZAP70* alleles revealed that the R360P mutation in ZAP70 results in increased downstream signaling events that leads to the expression of the activation marker CD69, suggesting that the R360P mutation functions as a weak hypermorphic allele in TCR signaling (14). The activation of the TCR pathway by the R360P allele is suppressed by the WT but not the R192W allele (14). Therefore, we speculate that our patients' disease likely results from increased TCR signaling due the hypermorphic R360P mutation. This phenotype is masked by WT ZAP70 as seen in the father and the unaffected sister and is revealed only in the presence of hypomorphic R192W allele as seen in the two affected siblings (14). However, it remains unclear how the R360P mutation affects T cell signaling and lymphocyte development in vivo. Because ZAP70 is mainly expressed in T and NK cells, the mechanisms by which the R360P mutation leads to a primarily antibody-mediated autoimmune syndrome is also unclear.

Here we showed that the biochemical signaling effects of the R360P mutation were consistent with weakening of the autoinhibitory conformation of ZAP70. *Zap70* R360P knock-in mice showed increased expansion of antigen-specific follicular helper T (Tfh) cells compared to that of the WT mice following LCMV infection. In addition, the R360P mutation was a weak hypermorphic allele of ZAP70 that enhanced TCR signaling. When introduced into the OTI TCR transgenic (tg) background, the R360P mutation sensitized TCR responses to weak and self peptides for the OTI TCR.

Results

The R360P mutation destabilizes the autoinhibitory conformation of ZAP70

Based on structural analysis, the R360P mutation was hypothesized to weaken the autoinhibited conformation of ZAP70 (Fig. 1A) (15). Mutations of Tyr^{315} and Tyr^{319} to Ala

(YYAA) in this region render ZAP70 constitutively active and lead to the phosphorylation of LAT, an important T cell signaling adaptor, even in the absence of Lck (15–17). In HEK293 cells, a modest degree of LAT phosphorylation was observed with coexpression of the full-length K362E ZAP70 mutant, but not with that of the full-length R360P ZAP70 mutant (14). We hypothesized that the possible activating effect of the R360P mutation on ZAP70 may be revealed in the absence of the SH2 domains and interdomain A that links these domains and participates in full autoinhibition (15). Immunoblotting showed marked LAT phosphorylation in cells expressing the YYAA ZAP70 mutant lacking the SH2 domain-interdomain A segment, as expected (Fig. 1B, C). We observed modest but apparent spontaneous LAT phosphorylation in cells expressing either the R360P or the K362E ZAP70 mutants lacking the SH2 domain-interdomain A segment (Fig. 1B, C). These results support the notion that the R360P mutation directly weakens ZAP70 autoinhibition, thereby rendering ZAP70 partially constitutively active.

Tolerance is preserved in ZAP70 R360P mice

To further understand how the ZAP70 R360P mutation affects TCR signaling, lymphocyte development, and promotes autoimmunity in human patients, we generated *Zap70* R360P knock-in mice on the C57BL/6 background using CRISPR-CAS9 technology. Initial founder mice were backcrossed to C57BL/6 mice for at least five generations to eliminate any potential off-target effects from CRISPR technology. The R360P mice were fertile, had normal life spans, and did not exhibit signs of increased morbidity compared with age and gender matched WT controls. In contrast to the patients with compound R360P/R192W ZAP70 mutations who developed a severe familial autoimmune syndrome early in life (14), the homozygous R360P mice did not develop any spontaneous autoimmune diseases based on histological screening of multiple organs from 8–10 month old mice (fig. S1). There was no evidence of lymphadenopathy or splenomegaly. Serologic screening for autoantibodies including ANA and dsDNA was negative.

T cell development and homeostasis were altered in ZAP70 R360P mice

We found that T cell development was comparable in young WT and R360P mice with polyclonal T cell repertoires. There were no substantial differences in overall cellularity in the thymuses, spleen and lymph nodes of R360P mice relative to WT mice (Fig. 2A). However, examination of peripheral T cell subsets showed that there was a substantial increase in the percentage of $CD44^{hi}CD62L^{hi}$ central memory $CD8^+$ T cells in the secondary lymphoid organs of 6–8 week old R360P mice compared to those of age-matched controls (Fig. 2B). Moreover, there was increased CD44 abundance on naïve $CD8^+$ T cell population (Fig. 2B). In addition, there was an increase in the percentage of $CD4^+CD25^+Foxp3^+$ T regulatory (Treg) cells in the lymph nodes of 6 month old R360P mice (Fig. 2C). Moreover, in activated $Foxp3^-CD44^{hi}CD4^+$ T cells, we observed an increase in the naturally occurring $CD73^{hi}FR4^{hi}$ anergic population, as defined by coexpression of CD73 and folate receptor 4 (FR4) (18), in aged R360P mice compared with WT mice (Fig. 2D). Together, these results suggest that T cells from R360P mice may exhibit enhanced TCR signaling, thereby leading to increases in the differentiation of CD8 memory T cells and Treg cells, and in the diversion to an anergic state.

The ZAP70 R360P functions as a weakly hypermorphic variant in the TCR signaling pathways

We next assessed whether TCR-induced downstream signaling events and activation responses were altered in R360P thymocytes or peripheral T cells. We found that there was no apparent difference in the surface TCRβ amounts between WT and R360P thymocytes subsets or peripheral T cells with polyclonal repertoire (fig. S2). By intracellular staining, we found that the R360P mutation caused ~30% reduction of ZAP70 protein in the thymocytes and peripheral T cells of homozygous R360P mice (Fig. 3A). Despite lower ZAP70 expression in R360P cells, the phosphorylation of Tyr^{319} in ZAP70 was modestly enhanced in R360P thymocytes compared to WT controls, both basally and following anti-CD3 stimulation (Fig. 3B). The enhancement of Tyr^{319} phosphorylation in R360P ZAP70 relative to that in WT ZAP70 was more evident if the amount of phosphorylated ZAP70 was standardized by the amount of total ZAP70 (Fig. 3B). This result is consistent with our hypothesis that the R360P mutation weakens the autoinhibitory conformation of ZAP70 which would sequester Tyr^{319} from accessibility for phosphorylation. The amounts of tyrosine-phosphorylated LAT, PLCγ, and Erk after TCR stimulation were comparable between WT and R360P thymocytes (Fig. 3B, fig. S3). However, when WT or mutant cells were barcoded with different fluorescence markers and stimulated with anti-CD3 in the same test tube, R360P double positive (DP) thymocytes exhibited increased maximum Ca^{2+} responses. R360P peripheral $CD4^+$ T cells exhibited modestly faster Ca^{2+} mobilization, whereas R360P peripheral $CD8^+$ T cells exhibited both consistently faster Ca^{2+} mobilization and increased maximal Ca^{2+} responses relative to those of WT cells (Fig. 3C, D). Together, these results suggest that in mice with a polyclonal TCR repertoire, the R360P mutation was not associated with detectable changes in T cell development, although there were increases in CD44 abundance, peripheral CD8 central memory T cells, Treg cells and anergic T cells with associated evidence of increased TCR signaling responses to TCR stimulation with anti-CD3 antibody. These results are consistent with our previous study that proposed that the R360P mutation was a weak hypermorphic allele that increased TCR signaling (14).

R360P mice exhibited expansion of T follicular helper (Tfh) cells.

Patients harboring the R360P ZAP70 allele developed autoantibody-mediated manifestations of disease (bullous pemphigoid and anti-factor VIII antibody) although ZAP70 is primarily expressed in T cells and NK cells (14). We hypothesized that the weakly hypermorphic R360P ZAP70 mutation resulted in excessive auto-reactive T helper cell activity for B cells, most likely mediated by Tfh cells, thereby leading to primarily autoantibody mediated manifestations as seen in our patients. To test this hypothesis, we assessed the effect of R360P mutant on the induction of Tfh cells in response to an acute infection with the Armstrong strain of lymphocytic choriomeningitis virus (LCMV). In the absence of LCMV infection, WT and the R360P mice exhibited similar percentages of Tfh cells among $CD4^+$ T cells in Peyer's patches (fig. S4, A and B). At day 8 after infection, the percentage of Tfh cells among $GP66^+$ antigen-specific effector cells ($B220^-CD4^+CD44^+GP66^+$) was significantly higher in R360P mice relative to that in WT mice (Fig. 4A). However, no significant difference was observed in germinal center (GC) B cell expansion or the anti-LCMV IgG antibody amounts between LCMV-infected WT and R360P mice (Fig. 4B, fig. S5, A and B). We next compared total immunoglobin amounts between WT and R360P

mice at various ages. Consistent with our findings of increased Tfh cell expansion in R360P mice, we found that there were substantial increases in IgG and IgG1 amounts in 10 month old R360P mice compared to those of WT controls (Fig. 4C, fig. S6). There was no difference in the total IgM amounts between WT and R360P mice at various ages (Fig. 4C). These findings suggest that the R360P ZAP70 mutation results in increased differentiation of or polarization towards antigen-specific Tfh cells in response to acute LCMV infection, possibly as a consequence of enhanced TCR signaling. Although the expansion in Tfh cells in R360P in mice with a polyclonal repertoire was insufficient to elicit enhanced numbers of GC B cells or higher anti-LCMV antibody titer in the acute LCMV infection model, the increase in total IgG amounts in aged R360P mice likely reflects a long term consequence of enhanced Tfh cell response.

The R360P mutation increases the response of T cells to low affinity ligands.

The increase in CD8 central memory T cells in the setting of grossly normal T cell development in R360P mice suggested that some compensatory mechanisms, such as a TCR repertoire shift, may have masked the effect of the R360P mutation on TCR signaling. To eliminate the effects of a possible repertoire shift, we crossed the R360P mice to C57BL/6 mice expressing the pOVA/MHCI-restricted OTI TCR transgene. Comparison of thymi from 8-week-old mice showed that thymic selection was not affected by the R360P mutation, even in the presence of the OTI transgene (Fig. 5A). The number of peripheral CD8-OTI T cells in R360P-OTI mice was also comparable to those in WT controls. Similar to R360P mice with a polyclonal TCR repertoire, we observed a substantial increase in the percentage of $CD44^{hi}CD62L^{hi}$ central memory $CD8^+$ T cells in the secondary lymphoid organs from the R360P-OTI mice relative to the controls (Fig. 5B). Additionally, the abundance of CD44 was ~ 50% higher on R360P CD8-OTI naïve T cells than that on WT cells (Fig. 5B), indicative of elevated basal signaling in R360P OTI T cells. Although the percentages of Vα2 clonotype-positive CD8SP thymocytes and peripheral $CD8^+$ T cells were comparable between WT and mutant mice (fig. S7A), TCR and Vα2 surface expression was consistently reduced on R360P CD8-OTI T cells (Fig. 6A). The differences were less apparent in CD8SP thymocytes (fig. S7B). In contrast, we did not observe differences in the TCR amounts on $CD8^+Vα2^-$ T cells from WT or R360P OTI mice. Additionally, TCR amounts were lower in R360P $CD8^+Vα2^+$ T cells when compared to R360P $CD8^+Vα2^-$ T cells (Fig. 6A). These results suggest that TCR recycling or degradation might be affected in the presence of R360P mutation, possibly due to a negative feedback compensatory mechanism driven by the enhanced tonic TCR signaling, which was better revealed by the introduction of OTI TCR.

It is possible that the expansion of $CD8^+$ T_{CM} resulted from a loss of the homeostatic regulation of naive T cells by self antigens or low-affinity antigens. We considered that the difference in the R360P mutation effect on TCR signaling downstream of ZAP70 may be revealed only with weak TCR stimuli but masked by a strong TCR stimulus such as high dose anti-CD3. To further examine whether the TCR activation threshold was affected by the R360P mutant allele, we utilized a panel of well-characterized altered chicken $ovalbumin_{257–264}$ (OVA) peptide ligands (APLs) presented by $H\text{-}2K^b$ MHC molecules, in which substitutions of one or two amino acids of the full agonist peptide OVA sequences

yields partial agonists or weak agonists for OTI TCR. As observed in cells with a polyclonal TCR repertoire, the basal phosphorylation of Tyr^{319} in ZAP70 was increased in R360P CD8-OTI cells compared to WT controls. Notably, although the phosphorylation of Tyr^{319} in ZAP70 was modestly increased in R360P CD8-OTI cells following stimulation with the strong agonist OVA, its phosphorylation was more markedly elevated in R360P CD8-OTI cells following stimulation with the weak antigen G4 relative to WT controls (Fig. 6B, C, fig. S8). When R360P or WT CD8-OTI T cells were stimulated by antigen presenting cells (APCs) preloaded with peptides of different agonist potency, we observed enhanced upregulation of the activation marker CD69 in R360P cells relative to that of WT cells in response to weak agonists (Q4H7 or G4), contrasting with only slight to no enhancement in the responses to strong agonists (OVA or Q4R7) (Fig. 6D). Neither R360P nor WT cells responded towards an unrelated peptide, VSV (Fig. 6D). Together, these results suggest that the R360P CD8-OTI T cells exhibited a lower ligand responsiveness threshold than did wild-type cells and, moreover, that the R360P allele selectively positively influenced responses to low affinity peptides.

The R360P mutation conferred enhanced T cell proliferation in response to low affinity and self antigens

We next sought to assess additional downstream functional effects of the R360P mutation following stimulation with strong or weak ligands. To do so, we assessed the effect of R360P mutation on TCR-induced proliferation in response to 2.5–3 days of peptide ligand stimulation as assessed by dilution of Cell Trace Violet (CTV) dye. Although the in vitro proliferation responses of R360P CD8-OTI cells to OVA were only slightly enhanced compared to those of WT cells, R360P CD8-OTI T cells exhibited more robust relative proliferative responses to the weak agonist G4 at suboptimal peptide doses for WT cells (Fig. 7A). Similar results were observed when the cells were cultured in the presence of exogenous IL-2 (Fig. 7A). Because the G4 peptide is considered to have an affinity in the range of positively selecting self-peptides (19–21), these results suggest that under certain antigen dosages and cytokine milieu, the R360P mutation may allow increased mature T cell sensitivity to self-antigens that would normally be ignored by T cells from WT mice.

We next investigated whether the R360P mutation may allow for increased T cell sensitivity to self-peptides by determining whether the R360P CD8-OTI cell would respond to the naturally occurring positively selecting self-peptides for OTI TCR, such as Catnb (which is derived from β-$catenin_{329–336}$) (22). In the absence of IL-2, neither WT nor R360P CD8-OTI T cells responded to Catnb. However, in the presence of IL-2, R360P CD8-OTI T cells exhibited a stronger proliferative response to Catnb, relative to the WT controls (Fig. 7B). Again, neither R360P nor WT cells responded towards an unrelated peptide, VSV (Fig. 7B). This result suggests that the R360P mutation may indeed allow for increased mature T cell sensitivity to self-antigens, particularly in the context of a susceptible cytokine milieu or under inflammatory conditions.

Discussion

In the present study, we characterized a mouse model carrying the *Zap70* R360P mutation. This mutation was thought to contribute to a familial autoimmune syndrome (14). In contrast to humans, R360P mice did not spontaneously develop a detectable autoimmune phenotype, which may be due to their genetic background. The C57BL/6 strain is relatively resistant to developing autoimmune diseases. Likewise, the presence of other genetic modifiers or environmental stimuli in the patients may contribute to their predisposition to autoimmunity in the setting of increased ZAP70 activity and resultant T cell sensitivity to weak antigens.

Structural analysis showed that the R360P mutation is located in the N-lobe of the catalytic domain of ZAP70 in a loop in close proximity to Tyr^{315} & Tyr^{319} and other C-terminal sequences of interdomain B (Fig. 1A). Thus, it is likely the mutation partially disrupts the autoinhibition of ZAP70. Indeed, we observed spontaneous LAT phosphorylation by the R360P ZAP70 mutant lacking SH2 domains-interdomain A segment in HEK293 cells. As predicted by this model, we found that Tyr^{319} phosphorylation was enhanced in the R360P mouse cells, both basally or following TCR stimulation. However, we failed to detect changes in thymocyte development but did detect evidence of perturbed TCR signaling and T cell function, including more memory, regulatory, and anergic T cells in R360P mice with a diverse TCR repertoire. Downstream TCR signaling events such as phosphorylation of LAT and Erk were not affected, but we showed a more rapid and increased Ca^{2+} response. Together, these results support the hypothesis that the R360P mutation is a weak hypermorph for TCR signaling.

In humans with ZAP70 deficiency, the predominant clinical feature is severe combined immunodeficiency, with little evidence of overt autoimmunity (14). ZAP70 is primarily expressed in T cells and NK cells. The familial autoimmune syndrome associated with the R360P ZAP70 mutation, however, has unique features of predominately autoantibody-associated autoimmunity. Our results showed that in the context of the OTI transgenic system, where compensation to increased TCR signaling by repertoire shift was not possible, enhanced T cell responses as a result of the R360P mutation was clearly revealed following TCR stimulation with weak and self peptides. These results suggest that the R360P mutation lowered the threshold for the TCR to respond to weak and self peptides, which may allow for increased T cell sensitivity to self antigens under certain systemic inflammatory environments in vivo, such as viral infections that commonly affect young children. Additionally, the R360P mutation led to an increase in Tfh polarization after LCMV infection and increases in total serum IgG and IgG1 amounts in aged mice. Tfh cells are essential for GC maturation and antibody affinity maturation. Altered $CD4^+$ T helper cell fate with polarization to Tfh cells is associated with multiple autoimmune diseases in humans and in mouse models due to dysregulated B cell responses (23–33). Therefore, our results provide a potential mechanism to explain how the R360P mutation in ZAP70 contributes to the break of B cell tolerance in our patients with familial autoimmune syndrome.

Our study further illustrates the importance of ZAP70 autoinhibition in maintaining appropriate T cell function and immune tolerance. In the non-phosphorylated state, Tyr^{315}

and Tyr^{319} are critical for stabilizing the inactive conformation of the ZAP70 kinase domain. Although the engagement of a doubly phosphorylated ITAM peptide by the tandem-SH2 domains of ZAP70 induces a substantial conformational change that releases the tandem-SH2 module and interdomain A, the activation of ZAP70 requires a second step to fully release autoinhibition. This second step involves phosphorylation of Tyr^{315} and Tyr^{319} by Lck, thereby disrupting the interaction between interdomain B with the N-terminal lobe of the catalytic domain and allowing the kinase to adopt an active conformation. Furthermore, the binding of the SH2 domain in Lck to Tyr^{319} stabilizes the active conformation of both ZAP70 and Lck, thereby establishing a potential positive feed forward loop (15, 17, 34, 35). Our previous work has shown that mutating both Tyr^{315} and Tyr^{319} to Ala (YYAA) in ZAP70 disrupts its autoinhibition and compromises the effector functions mediated by phosphorylated Tyr^{315} and Tyr^{319} (12). YYAA mice exhibit defects in thymic positive and negative selection, diminished TCR signaling, and produce rheumatoid factor following fungal challenge. Another ZAP70 mutation, W131A, disrupts the interdomain A-interdomain B interaction, therefore bypassing the first step in relieving autoinhibition, a role played by phospho-ITAM binding. W131A-OTII $CD4^+$ T cells exhibit enhanced basal TCR signaling but are hypo-responsive to TCR stimulation. This phenotype is at least partially due to marked induction of inhibitory receptors, acquisition of an anergic phenotype and an associated large expansion of Treg cells. In contrast to the W131A mutation, the R360P mutation bypasses the second step by weakly relieving the second step of autoinhibition, a role played by phosphorylation of Tyr^{315} and Tyr^{319} by Lck. Our results showed that disruption of ZAP-70 autoinhibition by the R360P mutation sensitized the TCR to weak and self peptides and polarized $CD4^+$ T helper cells to Tfh. These findings provide insights into the importance of maintaining the ZAP70 autoinhibitory conformation in regulating TCR ligand discrimination and $CD4^+$ T helper cell fate decision. Such regulation is essential for inducing protective immunity and restraining potentially damaging inflammatory responses to self antigens. In summary, by studying the ZAP70 R360P mutation that is associated with a severe familial autoimmune syndrome, our results expand our knowledge on how ZAP70 hypermorphic defects and interference in normal regulatory mechanisms of TCR signaling may contribute to human autoimmune diseases.

Materials and Methods

Generation of Zap70 R360P mice

Zap70 R360P knock-in mice were generated using CRISPR technology by the Gladstone Institutes Transgenic Gene Targeting Core facility. The sequence for the sgRNA used is 5'-TCGCATGCGCAAGTATGGCGGGG-3'. A 110 bp ssDNA oligo equally spanning the desired mutation site was used as repair template: CGAGCTTGGCTGTGGCAACTTTGGCTCCGTGC GCCAGGGAGTCTATCGCATGCCCAAGTATGGCGGCGC CTT CTG CCA CAG CGTGGGTAT CAGAGCAGAGGAGTTGTAGG. The sgRNA, DNA oligo, and CAS9 protein (PNA bio) were mixed and injected into zygotes from C57BL/6 mice. The injected zygotes were then transferred to surrogate mothers. A total of 29 pups were born, among which 2 pups carried the heterozygous R360P mutation. One pup also carried a second mutation in the intron immediately following R360. The pup with only the desired R360P

mutation was used as the founder mouse. The founder mouse was backcrossed to C57BL/6 mice for at least 5 generations to minimize off target effects from CRISPR. The mice were then bred into homozygous R360P mice. The primers used for genotyping were as follows: forward primer for wild type allele: 5'-AGGGAGTCTATCGCATGCGC-3'; forward primer for R360P allele: 5'- AGGGAGTCTATCGCATGCCC-3'; common reverse primer: 5'-AGCAGGAACTTGTGCAGGG-3'. The annealing temperature for the PCR reaction was 68.5°C. The size of the PCR product is 592bp.

Mice and cell line

All mice were bred and maintained in a specific pathogen-free facility and all studies were done according to the Institutional Animal Care and Use Committee guidelines of the University of California, San Francisco. WT C57BL/6 OTI TCR transgenic mice were purchased from The Jackson Laboratory. R360P OTI mice were generated in our laboratory by crossing OTI mice with R360P mice. Both male and female mice were used in experiments. HEK293 cells were obtained from the ATCC and were maintained in DMEM supplemented with 5% FBS and 2 mM glutamine.

Antibodies

The following antibodies were used for staining: CD4 BUV395, CD8α BUV737 (BD); CD5 PerCp-Cy5.5, CD25 PE or APC, CD44 FITC or Pacific Blue, CD45.2 PE, CD62L APC, CD69 APC, TCRβ Pacific Blue, Vα2 PE or Pacific Blue, CXCR5-biotin, PD-1 FITC, SLAM PE-Cy7, CD95 PE-Cy7, GL-7 FITC (Biolegend); B220 efluore780, CD8α efluore780, ZAP70 Alexa488, Strepavidin-A647 (Life Technology); GP66 tetramer PE or APC (NIH Tetramer Core Facility). The following antibodies were used for immunoblot analysis: ZAP70 (clone 1E7.2) (36); ZAP70-pTyr^{319} (clone 65E4), LAT-pTyr^{191}, Erk1/2, Erk1/2-pThr^{202}/pTyr^{204}, and PLCγ-pTyr^{183}, all from Cell Signaling Technology; anti-phosphotyrosine (4G10), PLCγ (Sigma-Aldrich), LAT (clone FL-233, Santa Cruz Biotechnology), FLAG (clone M2, Sigma-Aldrich), and GAPDH (clone 6C5, Santa Cruz Biotechnology).

Plasmid constructs and protein detection

WT ZAP70 cDNA lacking SH2 domains and mutants R360P, K362E, and YYAA (14, 16, 37) (prepared with Agilent site-directed mutagenesis kits) in vector pcDNA3 (Invitrogen) (0.1ug), and pEF FLAG-tagged LAT (2.2ug) were expressed in HEK293 cells (6-well plate) using Lipofectamine 2000 reagents (Invitrogen) according to the manufacturer's protocol. After 24 hours, cells were harvested, rinsed, and lysed on ice with 1% NP40 lysis buffer. Immunoblot analysis were performed as described below using monoclonal 1E7.2 (anti-ZAP70), 4G10 (anti-phosphotyrosine), and M2 (anti-FLAG; Sigma-Aldrich) antibodies.

Immunoblot analysis

Thymocytes isolated from WT or R360P mice were washed with PBS and rested for 30 min at 37°C. Cells were left unstimulated or stimulated with anti-CD3 (clone 2C11) at 37°C over time as described in each experiment. Peripheral CD8-OTI T cells were isolated from WT or R360P-OTI mice by negative depletion, incubated with OVA or G4 peptide tetramers (NIH

Tetramer Core Facility) in PBS for 15min on ice, and transferred to 37°C for stimulation over time as described. Cells were lysed with lysis buffer with a final concentration of 1% NP40 (containing inhibitors of 2 mM NaVO4, 10 mM NaF, 5 mM EDTA, 2 mM PMSF, 10 μg/ml Aprotinin, 1 μg/ml Pepstatin and 1 μg/ml Leupeptin). For cell line experiments, HEK293 cells were harvested and lysed 24 hours after transfection.

Lysates were placed on ice and centrifuged at 13,000 × g to pellet cell debris. Supernatants were run on NuPAGE 4%–12% Bis-Tris Protein Gels (Thermo Fisher Scientific) and transferred to PVDF membranes. Membranes were blocked using TBS-T buffer containing 3% BSA, and probed with primary antibodies as described in each experiment, overnight at 4°C. The following day blots were rinsed and incubated with HRP-conjugated secondary antibodies (Southern biotech). Blots were developed using a chemiluminescent substrate and a BioRad Chemi-Doc imaging system (Bio-Rad).

Ca^{2+} flux assay

Thymocytes or peripheral T cells from either WT or R360P mice were first loaded with 1 μM Indo-1 dye (Invitrogen) for 30 min at 37°C in RPMI medium plus 10% fetal bovine serum. After loading with Indo-1, cells were surface stained with anti-CD4 and anti-CD8 antibodies for subsequent identification of thymocytes or T cell subsets, as well as anti–CD45.2-PE for either WT or R360P cells for subsequent identification of the two genotypes. Cells from both genotypes were mixed together and analyzed by flow cytometry (Fortessa [BD] with a UV laser). Cells were stimulated with 10 μg/ml anti-CD3, followed by cross-linking with 50 μg/ml goat anti–Armenian hamster IgG (Jackson laboratory) at 37°C. Ca^{2+} increase was monitored as the ratio of Indo-1(blue) and indo-1(violet) and displayed as a function of time. Ionomycin was added at 220–230s to serve as a positive control.

LCMV infection

WT or R360P mice were infected intraperitoneally with 2×10^5 pfu of the Armstrong strain of LCMV virus. On day 8 post-infection, spleens were harvested for flow cytometry analysis.

ELISA

Serum LCMV-specific IgG and serum total immunoglobulin were measured by ELISA. For measuring serum anti-LCMV IgG, 96-well flat-bottom plates were coated with LCMV-infected BHK lysate and then blocked with PBS containing 0.5% Tween 20 (Bio-Rad) and 10% FBS. After blocking, serially diluted sera were added, and anti-mouse IgG conjugated to HRP (Southern Biotech) was used as the secondary antibody. To measure total serum immunoglobulin amounts, 96-well flat-bottom plates were coated with 1 μg/ml anti-mouse IgM, IgG or IgG subclasses (Southern Biotech). After blocking with PBS containing 0.05% Tween 20 and 1% BSA, serially diluted sera were added, and total immunoglobulin amounts were detected with anti-mouse IgM, IgG or IgG subclasses conjugated to HRP (Southern Biotech). Unlabeled mouse IgM, IgG or IgG subclasses (Southern Biotech) were used as standards. All ELISA plates were developed with 3,3′,5,5′-tetramethylbenzidine (Sigma-Aldrich) and stopped with 2N sulfuric acid. Absorbance was measured at 450 nm.

CD69 up-regulation assay

Sorted naive $CD8^+$ OTI T cells ($CD8^+V\alpha2^+CD44^-CD62L^+$) were incubated with *Calpha*$^{-/-}$ splenocytes at 1:5 ratio, preloaded for 1 hour with a series of titrated concentrations of OVA or APL peptides. Around 16 hours after stimulation, cells were fixed and stained for CD69, TCR Vα2, and CD8 and analyzed by flow cytometry.

In vitro proliferation assay

Sorted naive $CD8^+$ OTI T cells ($CD8^+V\alpha2^+CD44^-CD62L^+$) were resuspended in PBS, labeled for 20 min at 37°C with 5 μM cell trace violet (Life Technologies), and quenched with RPMI with 10% fetal bovine serum. Labeled $CD8^+$ OTI T cells were stimulated by antigen presenting cells (from *Calpha*$^{-/-}$ splenocytes) preloaded with a series of titrated concentrations of OVA, G4, or β-catenin$_{329–336}$, in the presence or absence of 50 units/ml IL-2. Cells were then subjected to flow cytometry analysis 2.5 −3 days after stimulation.

Statistical analysis

Paired or unpaired two-tailed Student's t tests were performed to determine statistical significance between two groups using Microsoft excel.

Supplementary Material

Refer to Web version on PubMed Central for supplementary material.

Acknowledgements:

We thank A. Roque (University of California, San Francisco) for animal husbandry, the NIH Tetramer Core Facility for providing the OVA and G4 peptide-loaded H-2K^b tetramers and GP66 tetramers, Z. Wang (University of California, San Francisco) for assistance with cell sorting, A. Chan (University of California, San Francisco) for technical advice, J. Zhang (Gladstone Institute Transgenic Gene Targeting Core) for assistance with generating R360P mice, and A. Mattis (University of California, San Francisco) for reviewing histology. We thank J. Zikherman, M. Anderson, J. Puck, W. Lo, and all Weiss lab members (all from University of California, San Francisco) for helpful suggestions on this project. We thank K. Taylor (University of California, San Francisco) for reviewing statistical analysis. **Funding:** The work was supported by the Rheumatology Research Foundation Scientist Development Award and K Bridge Award (to L.S.), NIH P01 AI091580 (to A.W.), and the Howard Hughes Medical Institute (to A.W.).

References and Notes

1. Liston A, Enders A, Siggs OM, Unravelling the association of partial T-cell immunodeficiency and immune dysregulation., Nat. Rev. Immunol 8, 545–558 (2008). [PubMed: 18551129]
2. Au-Yeung BB, Shah NH, Shen L, Weiss A, ZAP-70 in Signaling, Biology, and Disease., Annu. Rev. Immunol 36, 127–156 (2018). [PubMed: 29237129]
3. Chan AC, Iwashima M, Turck CW, Weiss A, ZAP-70: a 70 kd protein-tyrosine kinase that associates with the TCR zeta chain., Cell 71, 649–662 (1992). [PubMed: 1423621]
4. Au-Yeung BB, Deindl S, Hsu L-Y, Palacios EH, Levin SE, Kuriyan J, Weiss A, The structure, regulation, and function of ZAP-70., Immunol. Rev 228, 41–57 (2009). [PubMed: 19290920]
5. Wang H, Kadlecek TA, Au-Yeung BB, Goodfellow HES, Hsu L-Y, Freedman TS, Weiss A, ZAP-70: an essential kinase in T-cell signaling., Cold Spring Harb. Perspect. Biol 2, a002279 (2010). [PubMed: 20452964]
6. Chakraborty AK, Weiss A, Insights into the initiation of TCR signaling., Nat. Immunol 15, 798–807 (2014). [PubMed: 25137454]

7. Chan AC, Kadlecek TA, Elder ME, Filipovich AH, Kuo WL, Iwashima M, Parslow TG, Weiss A, ZAP-70 deficiency in an autosomal recessive form of severe combined immunodeficiency., Science 264, 1599–1601 (1994). [PubMed: 8202713]
8. Elder ME, Lin D, Clever J, Chan AC, Hope TJ, Weiss A, Parslow TG, Human severe combined immunodeficiency due to a defect in ZAP-70, a T cell tyrosine kinase., Science 264, 1596–1599 (1994). [PubMed: 8202712]
9. Negishi I, Motoyama N, Nakayama K, Nakayama K, Senju S, Hatakeyama S, Zhang Q, Chan AC, Loh DY, Essential role for ZAP-70 in both positive and negative selection of thymocytes., Nature 376, 435–438 (1995). [PubMed: 7630421]
10. Arpaia E, Shahar M, Dadi H, Cohen A, Roifman CM, Defective T cell receptor signaling and CD8+ thymic selection in humans lacking zap-70 kinase., Cell 76, 947–958 (1994). [PubMed: 8124727]
11. Sakaguchi N, Takahashi T, Hata H, Nomura T, Tagami T, Yamazaki S, Sakihama T, Matsutani T, Negishi I, Nakatsuru S, Sakaguchi S, Altered thymic T-cell selection due to a mutation of the ZAP-70 gene causes autoimmune arthritis in mice., Nature 426, 454–460 (2003). [PubMed: 14647385]
12. Hsu L-Y, Tan YX, Xiao Z, Malissen M, Weiss A, A hypomorphic allele of ZAP-70 reveals a distinct thymic threshold for autoimmune disease versus autoimmune reactivity., J. Exp. Med 206, 2527–2541 (2009). [PubMed: 19841086]
13. Siggs OM, Miosge LA, Yates AL, Kucharska EM, Sheahan D, Brdicka T, Weiss A, Liston A, Goodnow CC, Opposing functions of the T cell receptor kinase ZAP-70 in immunity and tolerance differentially titrate in response to nucleotide substitutions., Immunity 27, 912–926 (2007). [PubMed: 18093540]
14. Chan AY, Punwani D, Kadlecek TA, Cowan MJ, Olson JL, Mathes EF, Sunderam U, Fu SM, Srinivasan R, Kuriyan J, Brenner SE, Weiss A, Puck JM, A novel human autoimmune syndrome caused by combined hypomorphic and activating mutations in ZAP-70., J. Exp. Med 213, 155–165 (2016). [PubMed: 26783323]
15. Yan Q, Barros T, Visperas PR, Deindl S, Kadlecek TA, Weiss A, Kuriyan J, Structural basis for activation of ZAP-70 by phosphorylation of the SH2-kinase linker., Mol. Cell. Biol 33, 2188–2201 (2013). [PubMed: 23530057]
16. Brdicka T, Kadlecek TA, Roose JP, Pastuszak AW, Weiss A, Intramolecular regulatory switch in ZAP-70: analogy with receptor tyrosine kinases., Mol. Cell. Biol 25, 4924–4933 (2005). [PubMed: 15923611]
17. Deindl S, Kadlecek TA, Brdicka T, Cao X, Weiss A, Kuriyan J, Structural basis for the inhibition of tyrosine kinase activity of ZAP-70., Cell 129, 735–746 (2007). [PubMed: 17512407]
18. Kalekar LA, Schmiel SE, Nandiwada SL, Lam WY, Barsness LO, Zhang N, Stritesky GL, Malhotra D, Pauken KE, Linehan JL, O'Sullivan MG, Fife BT, Hogquist KA, Jenkins MK, Mueller DL, CD4(+) T cell anergy prevents autoimmunity and generates regulatory T cell precursors., Nat. Immunol 17, 304–314 (2016). [PubMed: 26829766]
19. Jameson SC, Hogquist KA, Bevan MJ, Specificity and flexibility in thymic selection., Nature 369, 750–752 (1994). [PubMed: 8008067]
20. Hogquist KA, Jameson SC, Heath WR, Howard JL, Bevan MJ, Carbone FR, T cell receptor antagonist peptides induce positive selection., Cell 76, 17–27 (1994). [PubMed: 8287475]
21. Hogquist KA, Jameson SC, Bevan MJ, Strong agonist ligands for the T cell receptor do not mediate positive selection of functional CD8+ T cells., Immunity 3, 79–86 (1995). [PubMed: 7621079]
22. Santori FR, Kieper WC, Brown SM, Lu Y, Neubert TA, Johnson KL, Naylor S, Vukmanović S, Hogquist KA, Jameson SC, Rare, structurally homologous self-peptides promote thymocyte positive selection., Immunity 17, 131–142 (2002). [PubMed: 12196285]
23. Crotty S, T follicular helper cell differentiation, function, and roles in disease., Immunity 41, 529–542 (2014). [PubMed: 25367570]
24. Vinuesa CG, Linterman MA, Yu D, MacLennan ICM, Follicular helper T cells., Annu. Rev. Immunol 34, 335–368 (2016). [PubMed: 26907215]

25. Simpson N, Gatenby PA, Wilson A, Malik S, Fulcher DA, Tangye SG, Manku H, Vyse TJ, Roncador G, Huttley GA, Goodnow CC, Vinuesa CG, Cook MC, Expansion of circulating T cells resembling follicular helper T cells is a fixed phenotype that identifies a subset of severe systemic lupus erythematosus., Arthritis Rheum. 62, 234–244 (2010). [PubMed: 20039395]
26. Liu R, Wu Q, Su D, Che N, Chen H, Geng L, Chen J, Chen W, Li X, Sun L, A regulatory effect of IL-21 on T follicular helper-like cell and B cell in rheumatoid arthritis., Arthritis Res. Ther 14, R255 (2012). [PubMed: 23176102]
27. Morita R, Schmitt N, Bentebibel S-E, Ranganathan R, Bourdery L, Zurawski G, Foucat E, Dullaers M, Oh S, Sabzghabaei N, Lavecchio EM, Punaro M, Pascual V, Banchereau J, Ueno H, Human blood CXCR5(+)CD4(+) T cells are counterparts of T follicular cells and contain specific subsets that differentially support antibody secretion., Immunity 34, 108–121 (2011). [PubMed: 21215658]
28. Choi J-Y, Ho JH, Pasoto SG, Bunin V, Kim ST, Carrasco S, Borba EF, Gonçalves CR, Costa PR, Kallas EG, Bonfa E, Craft J, Circulating follicular helper-like T cells in systemic lupus erythematosus: association with disease activity., Arthritis Rheumatol. 67, 988–999 (2015). [PubMed: 25581113]
29. Akiyama M, Suzuki K, Yamaoka K, Yasuoka H, Takeshita M, Kaneko Y, Kondo H, Kassai Y, Miyazaki T, Morita R, Yoshimura A, Takeuchi T, Number of Circulating Follicular Helper 2 T Cells Correlates With IgG4 and Interleukin-4 Levels and Plasmablast Numbers in IgG4-Related Disease., Arthritis Rheumatol. 67, 2476–2481 (2015). [PubMed: 25989153]
30. Vinuesa CG, Cook MC, Angelucci C, Athanasopoulos V, Rui L, Hill KM, Yu D, Domaschenz H, Whittle B, Lambe T, Roberts IS, Copley RR, Bell JI, Cornall RJ, Goodnow CC, A RING-type ubiquitin ligase family member required to repress follicular helper T cells and autoimmunity., Nature 435, 452–458 (2005). [PubMed: 15917799]
31. Linterman MA, Rigby RJ, Wong RK, Yu D, Brink R, Cannons JL, Schwartzberg PL, Cook MC, Walters GD, Vinuesa CG, Follicular helper T cells are required for systemic autoimmunity., J. Exp. Med 206, 561–576 (2009). [PubMed: 19221396]
32. Lee SK, Silva DG, Martin JL, Pratama A, Hu X, Chang P-P, Walters G, Vinuesa CG, Interferon-γ excess leads to pathogenic accumulation of follicular helper T cells and germinal centers., Immunity 37, 880–892 (2012). [PubMed: 23159227]
33. Bubier JA, Sproule TJ, Foreman O, Spolski R, Shaffer DJ, Morse HC, Leonard WJ, Roopenian DC, A critical role for IL-21 receptor signaling in the pathogenesis of systemic lupus erythematosus in BXSB-Yaa mice., Proc. Natl. Acad. Sci. USA 106, 1518–1523 (2009). [PubMed: 19164519]
34. Klammt C, Novotná L, Li DT, Wolf M, Blount A, Zhang K, Fitchett JR, Lillemeier BF, T cell receptor dwell times control the kinase activity of Zap70., Nat. Immunol 16, 961–969 (2015). [PubMed: 26237552]
35. Thill PA, Weiss A, Chakraborty AK, Phosphorylation of a tyrosine residue on zap70 by lck and its subsequent binding via an SH2 domain may be a key gatekeeper of T cell receptor signaling in vivo., Mol. Cell. Biol 36, 2396–2402 (2016). [PubMed: 27354065]
36. Qian D, Lev S, van Oers NS, Dikic I, Schlessinger J, Weiss A, Tyrosine phosphorylation of Pyk2 is selectively regulated by Fyn during TCR signaling., J. Exp. Med 185, 1253–1259 (1997). [PubMed: 9104812]
37. Deindl S, Kadlecek TA, Cao X, Kuriyan J, Weiss A, Stability of an autoinhibitory interface in the structure of the tyrosine kinase ZAP-70 impacts T cell receptor response., Proc. Natl. Acad. Sci. USA 106, 20699–20704 (2009). [PubMed: 19920178]

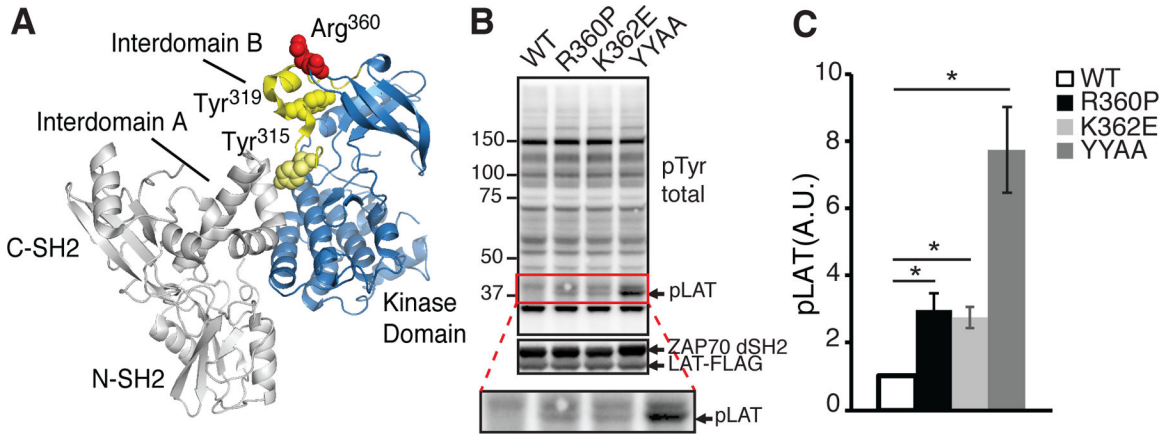

Figure 1. The R360P mutation weakens ZAP70 autoinhibition.

(A) Protein structure of ZAP70 (PDB 4K2R), highlighting residues (Tyr^{315} and Tyr^{319}) that participate in autoinhibition with yellow spheres. R360 (red spheres), mutated in our patients, lies in the autoinhibitory region in close proximity to Tyr^{319} in the interdomain B segment (shown in yellow). Not depicted are segments of interdomain B (between the C-SH2 domain and resolved segment of interdomain B) or the activation loop of the catalytic domain. These segments were not resolved in the crystal structure. (B) Immunoblots of whole cell lysates from HEK293 cells transfected with LAT-FLAG and WT and the indicated ZAP70 mutants lacking the SH2 domains-interdomain A segment (ZAP70 dSH2). (top) pTyr (4G10) blotting to show phosphorylated LAT (lower band). (middle) Expression of ZAP70 dSH2 and LAT. (bottom) enlargement of the pTyr blot area marked with the red square. (C) The band densities of phosphorylated LAT are shown. Data were standardized to the band density of the WT control. Quantified data are summarized from four independent experiments. Error bars represent SEM. * $P<0.05$. Paired student's t-test was used to compare the amount of phosphorylated LAT in cells transfected with each of the ZAP70 mutant construct with the WT control. A.U.: arbitrary unit.

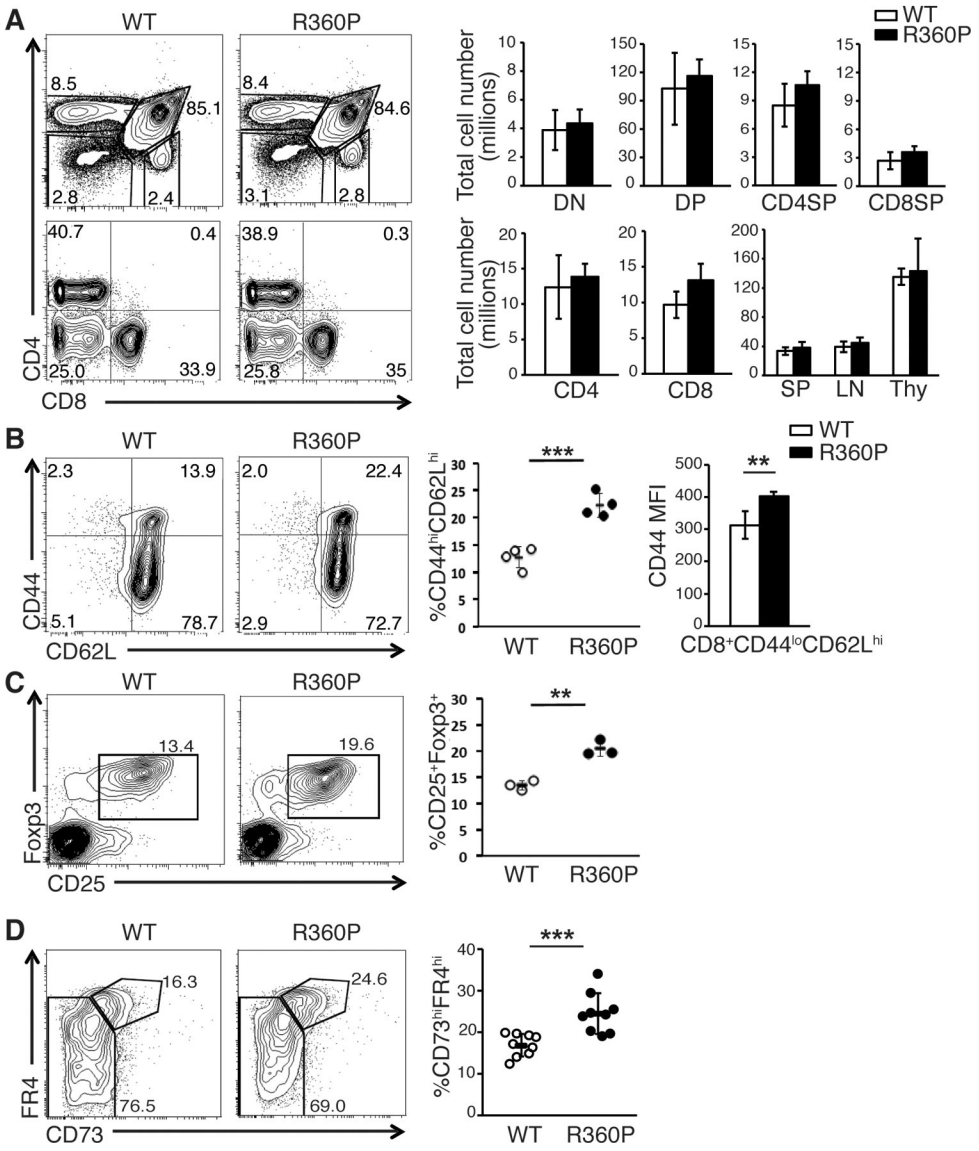

Figure 2. R360P mice with a polyclonal TCR repertoire have grossly normal T cell development and weakly enhanced TCR signaling.

(A) CD4 versus CD8 profiles of thymocytes (top) and lymph node (LN) cells (bottom) from WT and R360P mice. Numbers in quadrants are the percentages of each thymocyte or peripheral T cell subset. Total cell numbers of thymocyte subsets (top, including double negative (DN), double positive (DP), CD4 single positive (CD4SP), and CD8 single positive (CD8SP) subsets) and peripheral T cell subsets (bottom, including peripheral $CD4^+$ and $CD8^+$ T cell subsets) in age-matched 8 week old WT and R360P mice are shown on the right. Total cell numbers of spleen, lymph nodes and thymocytes from WT or R360P mice are also shown (n = 4 mice per group). (B) Comparison of central memory ($CD44^{hi}CD62L^{hi}$) T cells in $CD8^+$ T cells in LNs from WT and R360P mice (8 weeks old, n = 4 mice per group) (left and center panels). The mean fluorescence intensity (MFI) of CD44 of $CD8^+CD44^{lo}CD62L^{hi}$ WT or R360P T cells were also shown (right panel). (C) Comparison of % of Treg cells ($CD25^+Foxp3^+$) in $CD4^+$ T cells in LNs from WT and

R360P mice (6 months old, n = 3 mice per group). Results in (A) to (C) are representative of at least three independent experiments. All error bars represent SD. (D) $CD4^{+}Foxp3^{-}CD44^{hi}$ (memory/activated, bottom) T cells from lymph nodes from either WT or R360P mice were stained for CD73 and FR4. Percentages in $CD73^{hi}FR4^{hi}$ gate are shown. Quantified data (right) are summarized from three independent experiments (mice age: 6–9 months old; n = 9 mice per group). Error bars represent SD. Unpaired student's t-test was used for all statistical analysis. * $P < 0.05$, ** $P < 0.01$, *** $P< 0.001$.

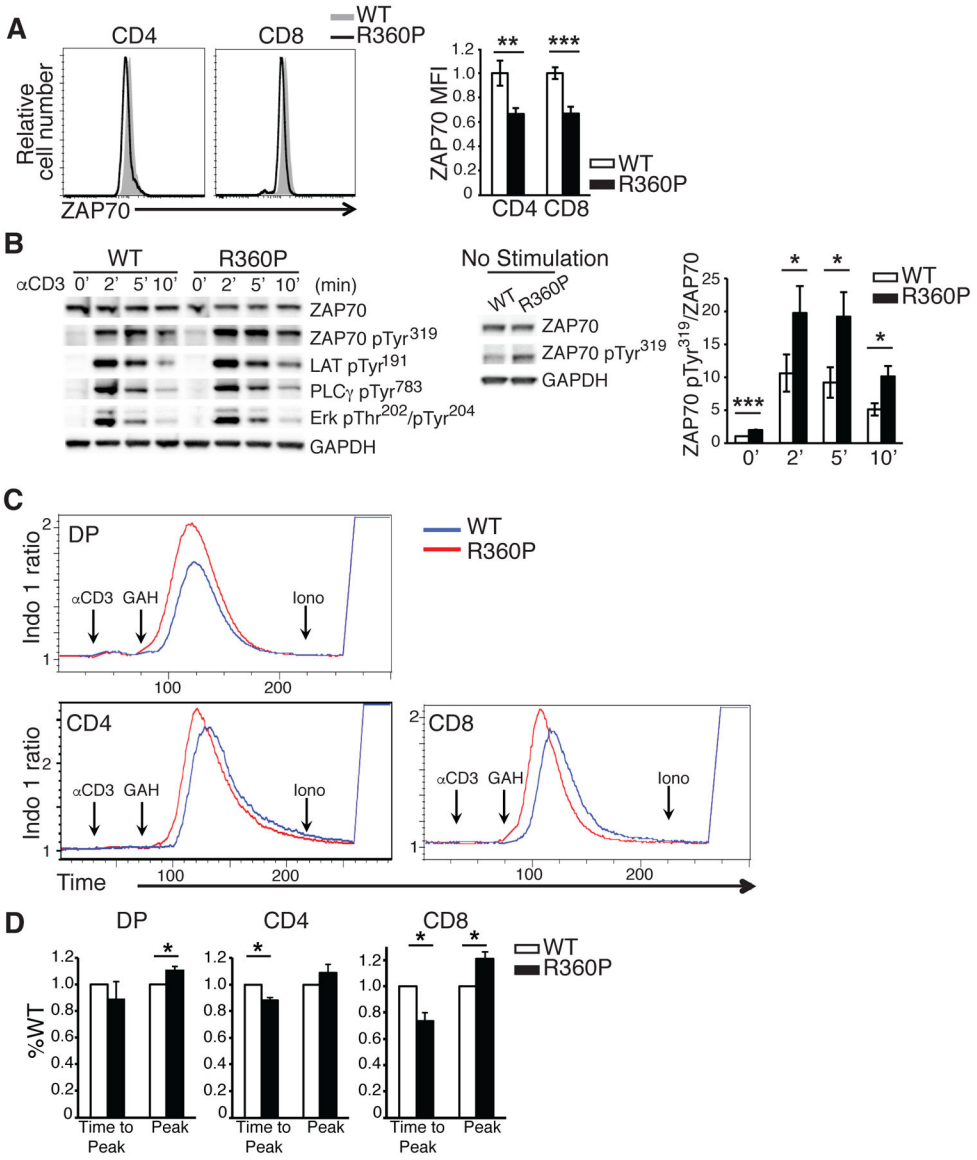

Figure 3. Effect of ZAP70 R360P mutation on T cell development and TCR signaling.

(A) ZAP70 amounts in peripheral $CD4^+$ or $CD8^+$ T cells from WT or R360P mice are shown. Error bars represent SD (n = 4 mice for WT, n = 3 mice for R360P). Data are representative of three independent experiments. Unpaired student's t-test was used for statistical analysis. (B) Thymocytes from WT or R360P mice were stimulated with anti-CD3 (2C11) antibody (10μg/ml) for the indicated times. Immunoblots of whole cell lysates with antibodies as labeled are shown on the left. The middle panel shows immunoblots of whole cell lysates of WT or R360P thymocytes at the basal state with antibodies as labeled. A long exposure was done for ZAP70-pTyr^{319}. The ratios of band density of ZAP70-pTyr^{319} standardized by total ZAP70 amounts from the above immunoblot analyses are shown on the right. Data are summarized from three independent experiments. Error bars represent SEM. Paired student's t-test was used for statistical analysis. GAPDH, glyceraldehyde-3-phosphate Dehydrogenase. (C) Ca^{2+} influx in double positive (DP) thymocytes, peripheral

$CD4^+$ or $CD8^+$ T cells from WT or R360P mice following TCR stimulation with anti-CD3 (2C11) (10μg/ml) and crosslinking with goat anti-Armenian hamster IgG (GAH) (50μg/ml); Iono: Ionomycin. (D) Bar graph showing the average peaks of Ca^{2+} influx (labeled as "peak"), as well as time taken to reach Ca^{2+} influx peak (labeled as "time to peak") from the time when GAH was added in DP thymocytes, peripheral $CD4^+$ or $CD8^+$ T cells. Data were standardized by the WT controls. Quantified data are summarized from three independent experiments. Error bars represent SD. Paired student's t-test were used for statistical analysis. * $P < 0.05$, ** $P < 0.01$, *** $P < 0.001$.

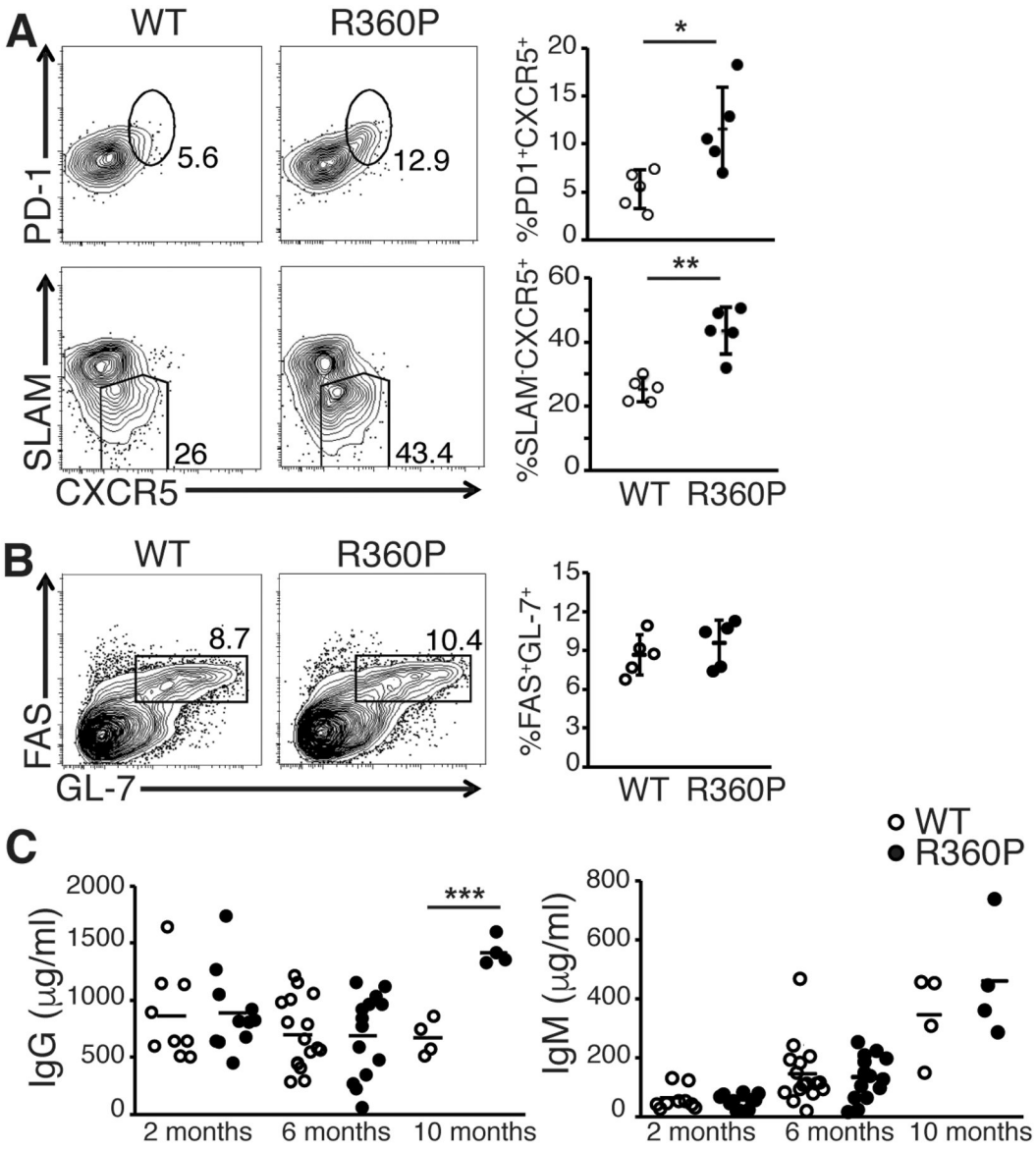

Figure 4. ZAP70 R360P mutation enhances antigen-specific Tfh cell differentiation and increases serum total immunoglobulin amount.

(A) Percentages of $CXCR5^+PD1^+$ or $CXCR5^+SLAM^{lo}$ Tfh cells 8 days following infecting WT or R360P mice with the Armstrong strain of LCMV. Results are gated on $B220^-CD4^+CD44^+GP66^+$ T cells from the spleen. (B) Percentages of FAS^+GL7^+ germinal center B cells among $B220^+$ cells from the spleen of WT or R360P mice 8 days following LCMV infection. Results are representative of at least three independent experiments. Error bars represent SD (n = 5 mice per group). (C) Serum total IgG and IgM amounts in WT or R360P mice at various ages as indicated. Data are summarized from at least three independent experiments (n = 4–16 mice per group). Unpaired student's t-test was used for statistical analysis. * $P < 0.05$, ** $P < 0.01$, and *** $P < 0.001$.

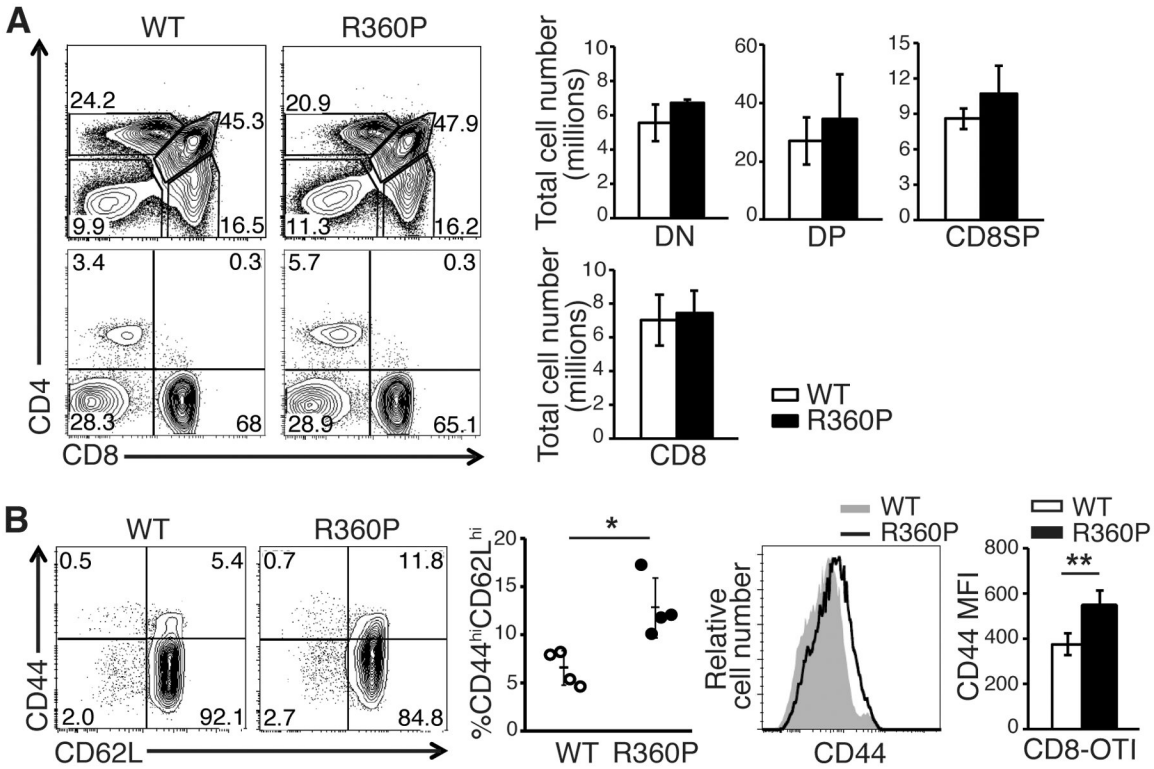

Figure 5. T cell development in R360P mice with OTI transgene.

(A) CD4 versus CD8 profiles of thymocytes (top) and LN cells (bottom) from WT and R360P mice. Numbers in quadrants are the percentages of each T cell subset. Total cell numbers in thymuses (top, including DN, DP, and CD8SP subsets) and LNs (bottom, peripheral $CD8^+$ T cells) in age-matched 8-week-old WT OTI and R360P OTI mice are shown on the right. (B) Comparison of % of $CD8^+$ OTI central memory ($CD44^{hi}CD62L^{hi}$) T cells in LNs from 8-week-old WT OTI and R360P OTI mice. The MFIs of CD44 of $CD8^+$ OTI WT or R360P T cells are also shown (right). All results are representative of at least three independent experiments. All error bars represent SD (n = 4 mice per group). Unpaired student's t-test was used for statistical analysis. * $P < 0.05$, ** $P < 0.01$.

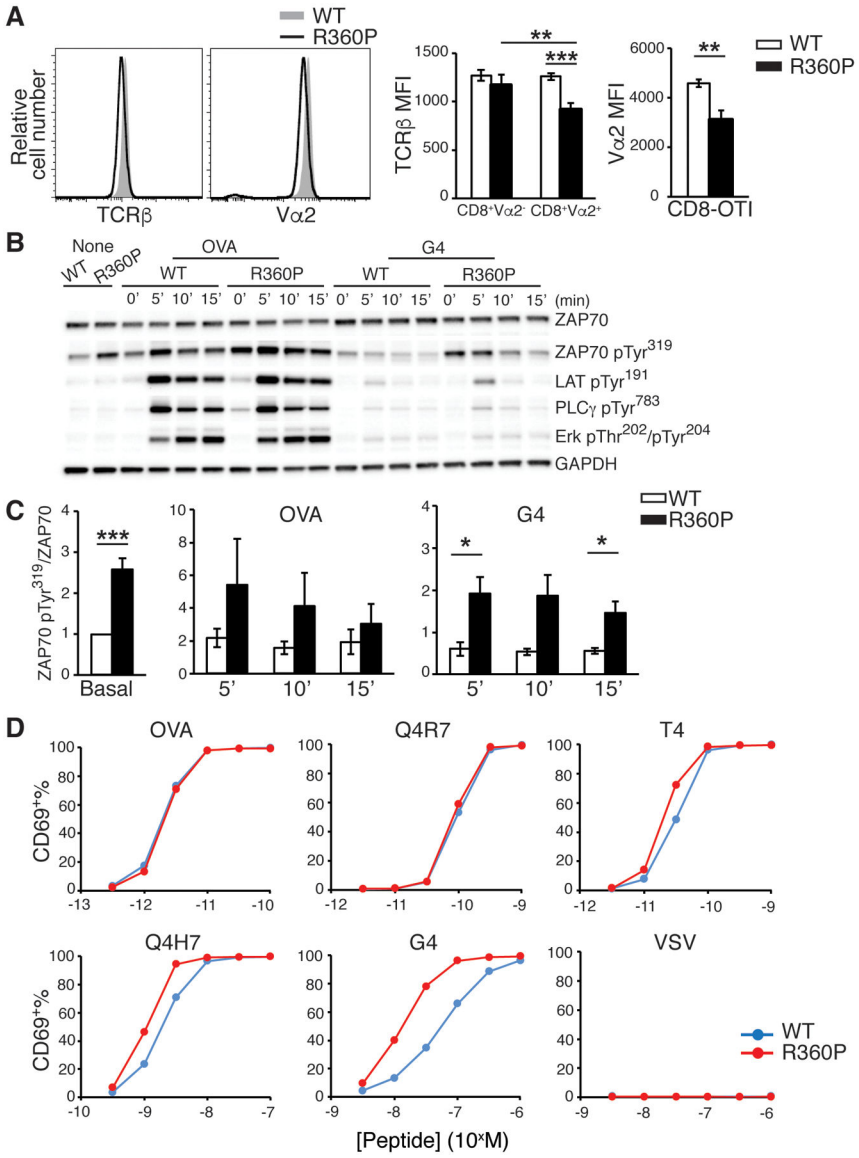

Figure 6. The R360P mutation in ZAP70 promotes T cells to respond to low-affinity antigen.

(A) TCRβ and Vα2 amounts on $CD8^+$ T cells from WT or R360P OTI mice. Error bars represent SD (n = 4 mice per group). Results are representative of at least three independent experiments. Unpaired student's t-test was used for statistical analysis. (B) Immunoblot analyses of purified $CD8^+$ T cells from WT OTI or R360P OTI mice that were left unstimulated or stimulated with either OVA or G4 (20μg/ml) for the indicated times. Graph is representative of three independent experiments. (C) The ratios of band density of ZAP70-$pTyr^{319}$ standardized to total ZAP70 amount from the immunoblot analyses in B are shown. Data are summarized from three independent experiments. Error bars represent SEM. Paired student's t-test was used for statistical analysis. (D) Percentages of CD69 positive $CD8^+$ OTI T cells following stimulation by antigen presenting cells pulsed with OVA peptide, OVA APL peptides, or VSV control peptide over the indicated peptide concentration ranges for 16 hours. Percentages of $CD69^+$ cells were plotted against peptide concentrations. Results are

representative of at least three independent experiments. * $P < 0.05$, ** $P < 0.01$, *** $P < 0.001$.

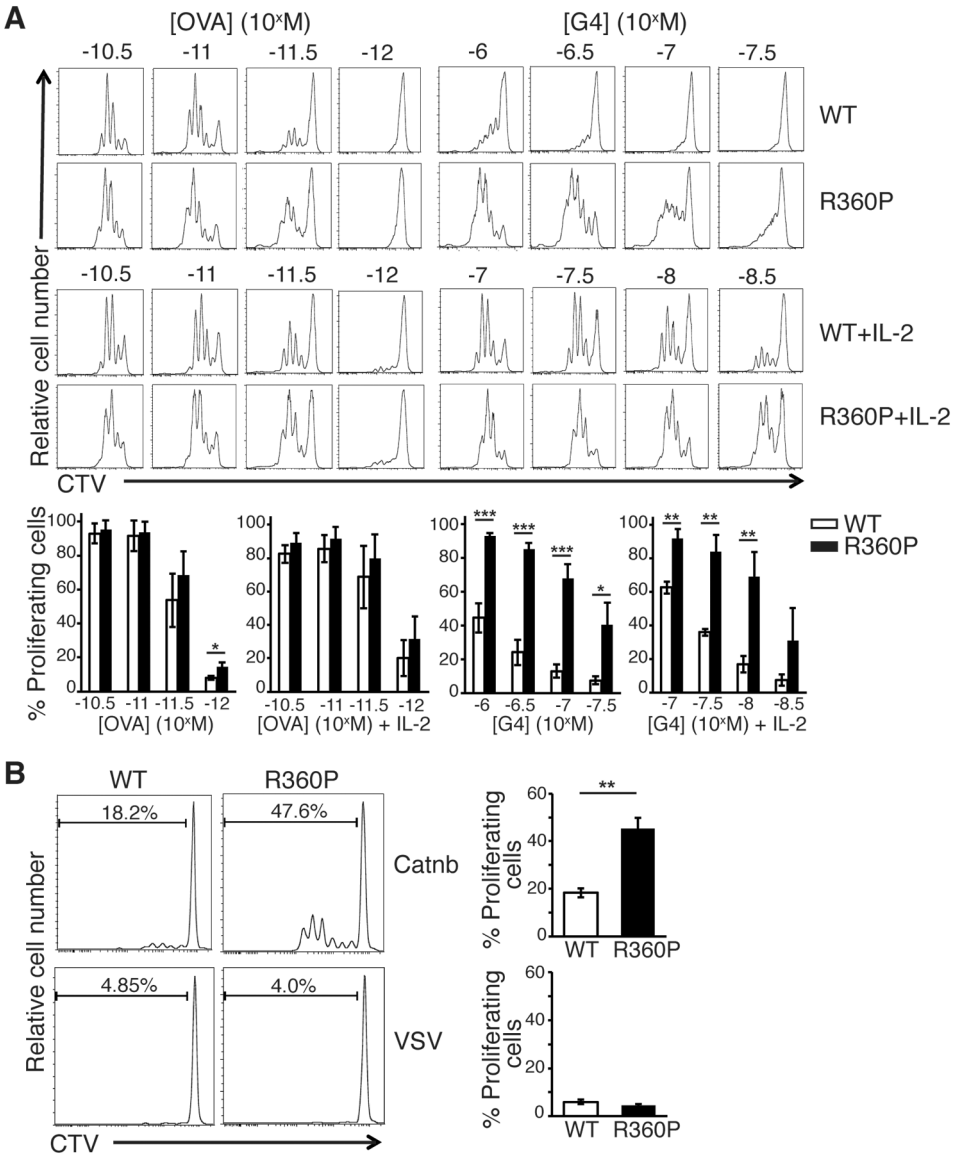

Figure 7. Enhanced proliferation of T cell from R360P OTI mice in response to low affinity and self antigens.

(A) In vitro proliferation of WT or R360P CD8$^+$ OTI T cells 2.5–3 days after stimulated by APCs preloaded with various concentrations of OVA or G4 peptide in the presence or absence of 50 unit/ml IL-2. Flow cytometry graph is representative of three independent experiments. % of proliferating cells are shown in the bar graph below. Quantified data are summarized from three independent experiments. Error bars represent SD. (B) In vitro proliferation of WT or R360P CD8$^+$ OTI T cells 2.5–3 days after stimulated by APCs preloaded with 30μM β-catenin$_{329–336}$ or VSV control peptide in the presence of 50 units/ml IL-2. CTV: cell trace violet. Data are representative of at least three independent experiments. Error bars represent SD. Unpaired student's t-test was used for statistical analysis. * $P < 0.05$, ** $P < 0.01$, *** $P < 0.001$.